Intracellular pH Response to Weak Acid Stress in Individual Vegetative Bacillus subtilis Cells

Pandey, R.; Vischer, N.O.E.; Smelt, J.P.P.M.; van Beilen, J.W.A.; Ter Beek, A.; De Vos, W.H.; Brul, S.; Manders, E.M.M.

DOI
10.1128/AEM.02063-16

Publication date
2016

Document Version
Final published version

Published in
Applied and Environmental Microbiology

License
Other

AMERICAN SOCIETY FOR MICROBIOLOGY | Applied and Environmental Microbiology

Intracellular pH Response to Weak Acid Stress in Individual Vegetative *Bacillus subtilis* Cells

Rachna Pandey,[a] Norbert O. E. Vischer,[a] Jan P. P. M. Smelt,[a] Johan W. A. van Beilen,[a] Alexander Ter Beek,[a] Winnok H. De Vos,[b,c] Stanley Brul,[a] Erik M. M. Manders[d]

Molecular Biology and Microbial Food Safety, SILS, University of Amsterdam, Amsterdam, The Netherlands[a]; Department of Veterinary Sciences, Laboratory of Cell Biology and Histology, Antwerp University, Antwerp, Belgium[b]; Department Molecular Biotechnology, Cell Systems and Imaging Group, Ghent University, Ghent, Belgium[c]; Van Leeuwenhoek Centre for Advance Microscopy, SILS, University of Amsterdam, Amsterdam, The Netherlands[d]

ABSTRACT

Intracellular pH (pH_i) critically affects bacterial cell physiology. Hence, a variety of food preservation strategies are aimed at perturbing pH_i homeostasis. Unfortunately, accurate pH_i quantification with existing methods is suboptimal, since measurements are averages across populations of cells, not taking into account interindividual heterogeneity. Yet, physiological heterogeneity in isogenic populations is well known to be responsible for differences in growth and division kinetics of cells in response to external stressors. To assess in this context the behavior of intracellular acidity, we have developed a robust method to quantify pH_i at single-cell levels in *Bacillus subtilis*. Bacilli spoil food, cause disease, and are well known for their ability to form highly stress-resistant spores. Using an improved version of the genetically encoded ratiometric pHluorin (IpHluorin), we have quantified pH_i in individual *B. subtilis* cells, cultured at an external pH of 6.4, in the absence or presence of weak acid stresses. In the presence of 3 mM potassium sorbate, a decrease in pH_i and an increase in the generation time of growing cells were observed. Similar effects were observed when cells were stressed with 25 mM potassium acetate. Time-resolved analysis of individual bacteria in growing colonies shows that after a transient pH decrease, long-term pH evolution is highly cell dependent. The heterogeneity at the single-cell level shows the existence of subpopulations that might be more resistant and contribute to population survival. Our approach contributes to an understanding of pH_i regulation in individual bacteria and may help scrutinizing effects of existing and novel food preservation strategies.

IMPORTANCE

This study shows how the physiological response to commonly used weak organic acid food preservatives, such as sorbic and acetic acids, can be measured at the single-cell level. These data are key to coupling often-observed single-cell heterogeneous growth behavior upon the addition of weak organic acid food preservatives. Generally, these data are gathered in the form of plate counting of samples incubated with the acids. Here, we visualize the underlying heterogeneity in cellular pH homeostasis, opening up avenues for mechanistic analyses of the heterogeneity in the weak acid stress response. Thus, microbial risk assessment can become more robust, widening the scope of use of these well-known weak organic acid food preservatives.

Microbes have evolved to maintain a narrow range of optimal intracellular pH (pH_i) values. For instance, under optimal growth conditions, *Bacillus subtilis* maintains its cytoplasmic pH at neutral or slightly higher values, with the exact range depending somewhat on the measurement tool used (compare data from reference 1 with our data). pH_i affects many biological processes, such as enzyme activity, reaction rates, protein stability, and the structure of different molecules, such as nucleic acids. Thus, the pH_i of bacteria is very important to ensure optimal growth, and conversely, perturbing the physiological pH_i is a strategy that is often exploited by the food industry for preservation purposes. Weak acids, such as sorbic, acetic, lactic, and benzoic acids, are naturally occurring preservatives that are commercially used in the food industry. These molecules are long known to inhibit the outgrowth of both bacterial and fungal cells (2), thereby allowing for the extension of the shelf-life of food products. Sorbic acid and its salts inhibit the growth of various bacteria, including spore-formers, at various stages of their life cycle, including spore germination, outgrowth, and vegetative cell division (3). The widely accepted theory of weak acid preservative action suggests inhibition of growth through lowering of the pH_i. According to the theory, undissociated acid molecules pass, depending on their lipophilicity, more or less readily through the plasma membrane by diffusion. In the cytoplasm (pH, >7.5), the acid molecules dissociate into charged anions and protons. These cannot pass across the lipid membrane and hence accumulate in the cytoplasm, lowering the pH_i of the cell. The acidification of the cytoplasm, in turn, inhibits metabolism. A recent study by van Beilen et al. (4) shows that sorbic acid has an ability to act as a classical uncoupler, transporting protons over the membrane, whereas acetic acid,

Received 13 July 2016 **Accepted** 21 August 2016

Accepted manuscript posted online 26 August 2016

Citation Pandey R, Vischer NOE, Smelt JPPM, van Beilen JWA, Ter Beek A, De Vos WH, Brul S, Manders EMM. 2016. Intracellular pH response to weak acid stress in individual vegetative *Bacillus subtilis* cells. Appl Environ Microbiol 82:6463–6471. doi:10.1128/AEM.02063-16.

Editor: D. W. Schaffner, Rutgers, The State University of New Jersey

Address correspondence to Stanley Brul, s.brul@uva.nl.

W.H.D.V., S.B., and E.M.M.M. contributed equally to this article.

Supplemental material for this article may be found at http://dx.doi.org/10.1128/AEM.02063-16.

which is less lipophilic, does so to a much lesser extent. This is corroborated by the fact that sorbic acid has a greater effect on the membrane potential, while acetic acid only carries bulk volume protons across the membrane until steady state is reached. Studies by Holyoak et al. (5) and Bracey et al. (6) showed that in *Saccharomyces cerevisiae*, the inhibitory action of weak acid preservatives evokes an energetically expensive stress response. This response in *S. cerevisiae* is based on a membrane-localized efflux system that removes both the accumulated anions as well as the excess protons from inside the cell (7, 8). The attempts to restore homeostasis, however, require significant amounts of ATP, resulting in a drop in available energy pools for growth and other essential metabolic functions. In summary, weak acids inhibit the growth of microbes in a number of ways, including through membrane perturbation, inhibition of essential metabolic reactions (3, 6), and stress on pH_i homeostasis (31), as well as the accumulation of toxic anions (6, 9).

Direct measurement of the pH_i may be used as a proxy for cellular metabolism and thereby provide rapid insight into survival strategies at the single-cell level. The pH_i of the cells can be measured by various methods, such as ^{31}P nuclear magnetic resonance (NMR), fluorescent dyes (most noticeably 5 [and 6-]-carboxyfluorescein diacetate succinimidyl ester) and the distribution of radiolabeled membrane-permeable weak acids (10–14). The advantage of these methods is that they do not require genetic modification. In the case of fluorescent dyes, single-cell measurements are possible (15). The disadvantage of using weak organic acid dyes is that they may themselves alter the pH_i. The disadvantage of the ^{31}P NMR and radiolabeled compounds is that they require extensive cell handling and high cell density, which also disturb the cell's physiology. Fluorescent proteins make an attractive and noninvasive alternative for measuring the pH_i of the bacterial cell, although obviously genetic modification is a prerequisite. pHluorin, a ratiometric and pH-sensitive green fluorescent protein (GFP) variant (16), allows direct, fast, and localized pH_i measurements. It has been successfully used in *S. cerevisiae* (17, 18) and more recently in *B. subtilis* (19–21) to probe cellular responses to various growth conditions, glucose pulses, respiratory chain inhibitors, and a few other treatments. A specific advantage of a fluorescence microscopy-based method is that it can provide information with (sub)cellular resolution (22, 23). This allows for the capturing of interindividual phenotypic heterogeneity that arises from factors, such as differential growth kinetics and stochastic effects, at the level of gene expression and protein activity. Taking advantage of this added value, we analyzed the effect of sorbic and acetic acid on the perturbation of the pH_i of *Bacillus subtilis* vegetative cells using an improved IpHluorin reporter.

MATERIALS AND METHODS

Growth conditions. To monitor the pH_i of exponentially growing *B. subtilis* cells for an extended period of time, the *B. subtilis* PptsG-IpHluorin (*trp2C amyE3′ spcR* P*ptsG-IpHluorin amyE5′*) construct was used (20). This construct consists of the pHluorin gene (16), which was inserted after the first 24 bp of *comGA* adjacent to the promoter PptsG, resulting in IpHluorin. This promoter drives the expression of the gene encoding the glucose-specific phosphotransferase system II. Thus, we were able to obtain expression of IpHluorin in vegetative cells growing on a glucose-containing medium. The *B. subtilis* 168 laboratory wild-type strain PB2 and *B. subtilis* PptsG-IpHluorin were grown exponentially in Luria broth (LB) at 37°C, under continuous agitation at 200 rpm. The exponentially growing cells were reinoculated in a minimal defined medium with 80 mM MOPS [3-(*N*-morpholino)propanesulfonic acid] (24), buffered to pH 7.4 (here referred to as MOPS medium). The MOPS medium contained spectinomycin (50 μg/ml) when appropriate, and cells were grown until exponential phase at 37°C, under continuous agitation at 200 rpm. The optical density at 600_{nm} (OD_{600}) was measured in time to determine if cells were in the exponential phase. Cells in the early exponential-growth phase (OD_{600}, ~0.2) were used for time-lapse microscopy experiments (see below). In stress experiments, 3 mM sorbic acid (KS) and 25 mM acetic acid (KAc) at pH 6.4 were used to test for their effect on the growth and pH_i of exponentially growing bacteria.

Phototoxicity measurements. Phototoxicity is a detrimental phenomenon in live-cell imaging, which occurs upon repeated exposure of fluorescently labeled cells to intense light. In order to test for possible phototoxicity, exponentially growing *B. subtilis* PB2 and *B. subtilis* PptsG-IpHluorin cells (grown in MOPS medium under live-imaging conditions, see below) were repetitively exposed to excitation light of two different wavelengths (390 nm and 470 nm) with exposure times of 100 ms and 30 ms, respectively, for a period of 5 h, with intervals of 5 min and 10 min. The exposure time was chosen in such a way that the bleaching in each channel has the same rate. The generation time of the cells was calculated with a home-written script for ImageJ (http://imagej.nih.gov/ij/) (25), Multichannel-SporeTracker. The total number of cells assessed for *B. subtilis* PB2 cells grown in the absence of fluorescent light was 107 and was between 77 and 164 for *B. subtilis* PptsG-IpHluorin cells cultured in the absence and presence of fluorescent light. The effect of phototoxicity on the cells was regarded as negligible when the generation times of vegetative cells did not differ significantly (*t* test, $P > 0.05$).

Fluorescence time-lapse microscopy (live imaging). In order to ensure the unbiased growth of aerobic bacteria, a closed air-containing chamber that has been described previously (25) was used for time-lapse fluorescence microscopy. In this chamber, cells were sandwiched between the glass coverslip and a thin (160 μm) 1% agarose-medium pad, molded in a Gene Frame, to ensure their immobilization in the presence of sufficient culture medium and enough oxygen for undisturbed growth. The pad was loaded with 1 μl of exponentially growing vegetative cells (OD_{600}, ~2). Time-lapse series were made by making use of a temperature-controlled boxed incubation system for live imaging set at 37°C.

The specimens were observed with a 100×/1.3 plane apochromatic oil objective mounted on a Zeiss wide-field fluorescence microscope (Axiovert-200; Zeiss, Jena, Germany) controlled by the MetaMorph 6.1 software. For ratiometric imaging, light from a Xenon arc lamp was filtered by a monochromator (OptoScan; Cairn Research Ltd., United Kingdom) and tuned to 390 nm or 470 nm, each with a bandwidth of 30 nm. The microscope was equipped with a standard GFP filter cube (Chroma) with 510-nm long-pass (LP) emission filter. Images were acquired with a CoolSnap HQ charge-coupled-device (CCD) camera (Roper Scientific). For phase-contrast imaging, a red filter (610 nm LP; Schott AG, Germany) was placed in the light path to protect the cells from phototoxicity. For control experiments, the time-lapse series of phase-contrast and fluorescence images were recorded at a sampling frequency of 1 frame per 10 min (see Results for the final choice of 10-min intervals) for 5 h, and for stress experiments, the cells were imaged for 10 h (also 1 frame per 10 min). Two biological replicates and 15 to 30 technical replicates (recorded fields of view on one slide) were recorded in parallel per experiment. In every field of view (technical replicate), 2 to 8 vegetative cells were identified and followed over time. This resulted in the analysis of approximately 30 to 60 vegetative cells from the start of each imaging experiment per biological replicate.

pH_i measurements in a microcolony and in single cells within a microcolony. For pH_i measurements, two image analyses tools for ImageJ were used. Multichannel-SporeTracker (https://sils.fnwi.uva.nl/bcb/objectj/examples/sporetracker/SporeTracker.htm) was developed for pH_i measurements at the microcolony level. This program runs in combination with ObjectJ (https://sils.fnwi.uva.nl/bcb/objectj/), a plugin for ImageJ. ObjectJ supports graphical vector objects that nondestruc-

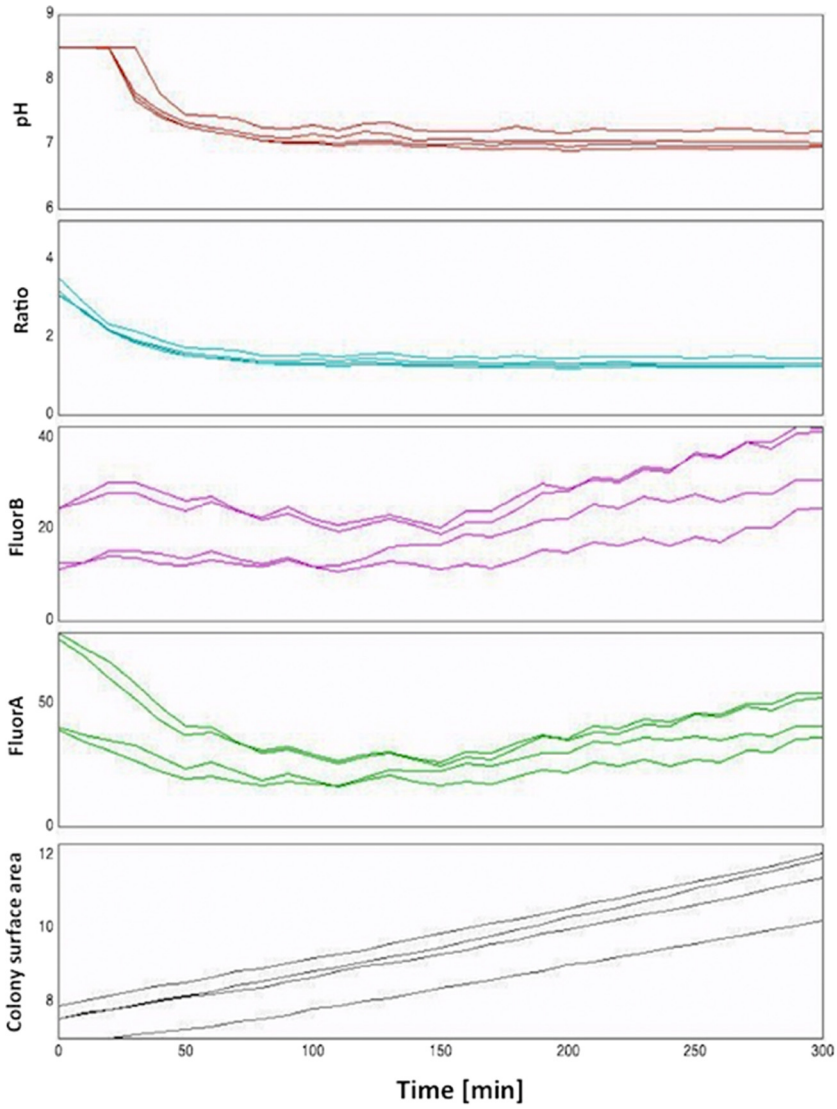

FIG 1 Multichannel-SporeTracker output for pH_i measurements in growing *B. subtilis* cells. Shown here are collective plots of 4 individual cells measured every 5 min for 5 h. Bottom to top: $\log_2$ (surface area occupied by cells); fluorescence intensities measured at 510 nm when excited at 390 nm (FluorA) and 470 nm (FluorB), respectively; and the ratio of the excitation wavelength (390 nm and 470 nm) of fluorescence intensities (2nd panel from the top) and pH_i (top). Note that here 4 cells are shown from the batch that starts at pH_i of >8; in cells from other batches pH_i was lower (~7.5) at the onset of imaging (see the text and Fig. 5 lineage tracking for comparison).

tively mark images on a transparent layer. It provides back-and-forth navigation between results and images. The results table supports statistics, sorting, color-coding, qualifying, and macro access.

Multichannel-SporeTracker allows accurate measurements of the intensity of IpHluorin in the cell, calculates the ratio (excitation at 390 nm [E_{390}]/E_{470}) of IpHluorin, and deduces the pH_i and the generation time of the vegetative cells growing into a microcolony at any desired time frame (Fig. 1). The generation time is calculated from the area ($\log_2$) of the growing cell population. The pH_i measurements are based on the ratio of the fluorescence emission at 510 nm after excitation at 390 nm and 470 nm, respectively (E_{390}/E_{470}). To calculate the pH_i, fluorescence images were first aligned with the corresponding phase-contrast images. Before measuring the fluorescence intensity of the cells, temporal intensity fluctuations were buffered by subtracting the mode (most frequent) value per frame throughout the time-lapse image stack. Then, the fluorescence intensities of IpHluorin-expressing cells were measured in both fluorescence channels within cellular regions of interest, and the E_{390}/E_{470} ratio was calculated. By correlating the ratio with a calibration curve (mentioned below), the pH_i of the cell was determined.

For pH_i measurements at the single-cell level, a custom-made script for IJ/FIJI ColiMetrics.ijm was used (https://www.uantwerpen.be/cell-group/). The algorithm segments individual bacteria and tracks them over time. It also converts the two-channel fluorescence image (excitation at 390 nm and 470 nm) into a color-coded image representing the pH_i for every individual cell in a microcolony (i.e., pH maps). pH_i maps are hue, saturation, value (HSV) images, in which the hue represents the ratio of both fluorescence channels, converted into a pH_i value according to a sigmoidal fit of the calibration curve, and the value is the average intensity of both channels (expansion of a macro described before; see reference 26). For single-cell analysis, individual bacteria were tracked over time up to the point of cell division. E_{390}/E_{470} ratios were measured per cell and plotted as a function of time.

Calibration of pH_i. *B. subtilis* PptsG-IpHluorin cells were grown to exponential phase in MOPS medium to pH 7.4 containing spectinomycin (50 μg/ml). At an OD_{600} of 0.4, the cells were centrifuged (1,073 × *g* for 10 min) and resuspended in phosphate-citrate buffers (0.1 M citrate and 0.2 M K_2HPO_4), with pH values ranging from 5.5 to 8.5, as described previously by us (20). The cells were then permeabilized with the potassium

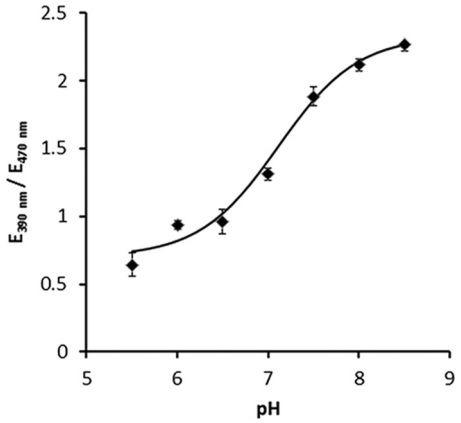

FIG 2 Calibration curve of *B. subtilis* PptsG-IpHluorin, which describes the relationship between the ratio of the emission intensity at 510 nm after excitation at 390 nm and 470 nm (E_{390}/E_{470}) and pH_i. The *B. subtilis* PptsG-IpHluorin cells were permeabilized using 1 μM nigericin and 1 μM valinomycin and immobilized on agarose pads containing both compounds at set pH values ranging from 5.5 to 8.5. The cell fluorescence emission intensities were measured, and the ratio (E_{390}/E_{470}) was plotted against pH_i. At least 200 cells were measured per data point. Error bars indicate the standard deviations. The figure gives a comparison between the observations (◆), including error bars (95% confidence limits of the observed values), and a fitted (✹) curve generated according to the Henderson-Hasselbalch equation. See the text for further details of the statistical analysis.

ionophore valinomycin (1 μM) and the protonophore nigericin (1 μM) (13). This treatment allows for the equilibration of the pH_i with the externally set pH. Subsequently, cells in the phosphate-citrate buffer of different pH (5.5 to 8.5) were transferred to agarose pads with the ionophores at 1 μM and of corresponding buffered pH values in closed air-containing chambers (20). For each pH, fluorescence images of ~200 cells were analyzed with Multichannel-SporeTracker to construct a calibration curve (Fig. 2). This curve represents the relationship between the ratio of the 510 nm emission intensities of IpHluorin upon excitation at 390 nm and 470 nm (E_{390}/E_{470}) and the pH_i.

The data were fitted to a slightly modified Henderson-Hasselbalch equation. It describes the relationship between the ratio of the intensity of wavelengths ($R = E_{390}/E_{470}$) and pH_i. Here, this was calculated as $R = ([10^{pHi - pKa}]/[10^{pHi - pKa} + 1]) \times b + a$. pK_a equals the $-\log_{10}$ of the dissociation constant, and b and a are parameters without physiological meaning, but they are used to enable a quantitative fit of the R values. The fitting procedure was conducted as follows: in total, 876 observations were available; 23 observations almost equally distributed across the different pH values were either negative of far beyond the set (3 standard deviations) to which they belonged. After elimination of these outliers, the average of each local clusters was taken. In total, 62 average values were obtained. To test the robustness of the model, 20 average values were selected randomly and left out. The 42 remaining values were fitted according to our modified Henderson-Hasselbalch equation. The estimates of the parameters, including confidence intervals, are shown in Tables 1 and 2. For nonlinear regression models, the correlation coefficients between the parameters can be considered acceptably low (27). The average residual sum of squares (RSS) was calculated for each pH value that was studied. No significant correlation was found between average RSS and pH. The average sum of squares was 0.00968.

TABLE 1 Parameter estimates of the slightly modified Henderson-Hasselbalch model (see "Calibration of pH_i" in Materials and Methods) describing the relationship between pH_i and the ratio of the IpHluorin fluorescence emission intensity upon excitation at 390/470 nm

Parameter	Estimate	SE	95% confidence interval	
			Lower bound	Upper bound
pK_a	7.112	0.055	7.001	7.223
b	1.625	0.048	1.528	1.722
a	0.703	0.040	0.621	0.785

TABLE 2 Correlations of parameter estimates reported in Table 1[a]

Parameter	pK_a	*b*	*a*
pK_a	1.000	−0.047	0.625
b	−0.047	1.000	−0.681
a	0.625	−0.681	1.000

[a] The average RSS was 0.00968.

RESULTS

Long-term ratiometric imaging of IpHluorin-expressing cells is not phototoxic. A typical fluorochrome can only withstand a limited number of excitation cycles. Excessive illumination eventually leads to irreversible loss of fluorescence (photobleaching) and the production of free radicals that can damage cellular components compromising cell viability (phototoxicity). The combined effect, i.e., photodamage, restricts long-term fluorescence live-cell imaging. Photodamage can be mitigated by the parsimonious use of illumination light but cannot be eliminated completely (28). To assess whether our imaging conditions allowed for monitoring bacterial cells without excessive photodamage, we compared the generation time with and without fluorescence illumination. In addition, we assessed the effect on cell growth of IpHluorin expression.

The generation time of wild-type *B. subtilis* PB2 cells grown in the absence of excitation light (93 ± 13 min) was similar to the generation time of the IpHluorin-expressing cells grown in the absence of excitation light (92 ± 17 min) (Fig. 3). Therefore, we concluded that IpHluorin expression is not harmful to the cells

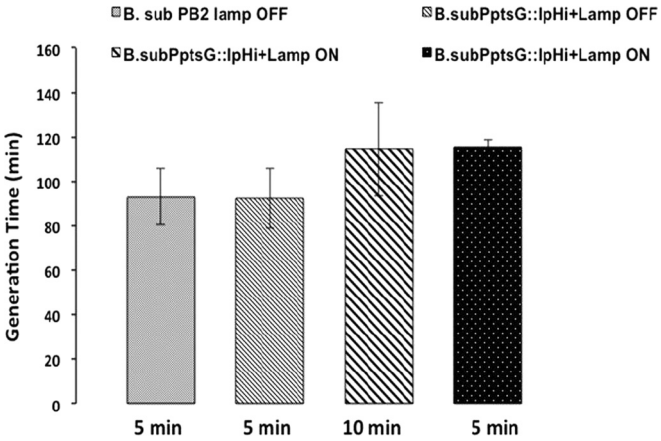

FIG 3 Effect of fluorescent light (excitation at 390 nm and 470 nm and emission at 510 nm) on *B. subtilis* PptsG-IpHluorin. Movies of *B. subtilis* PB2 cells grown in the absence of fluorescent light and *B. subtilis* PptsG-IpHluorin cells in the absence and presence of fluorescent excitation light (390 nm and 470 nm) with a time interval of either 5 min or 10 min were made during 5 h. Generation time was analyzed by Multichannel-SporeTracker. The total number of cells assessed for *B. subtilis* PB2 cells grown in the absence of fluorescent light was 107; for *B. subtilis* PptsG-IpHluorin cells in the absence of fluorescent light, it was 164; and for regularly illuminated PptsG-IpHluorin cells, it was 77 (for the specimens inspected every 10 min) and 92 (for those illuminated every 5 min). No cell lysis was observed while analyzing either of the incubations.

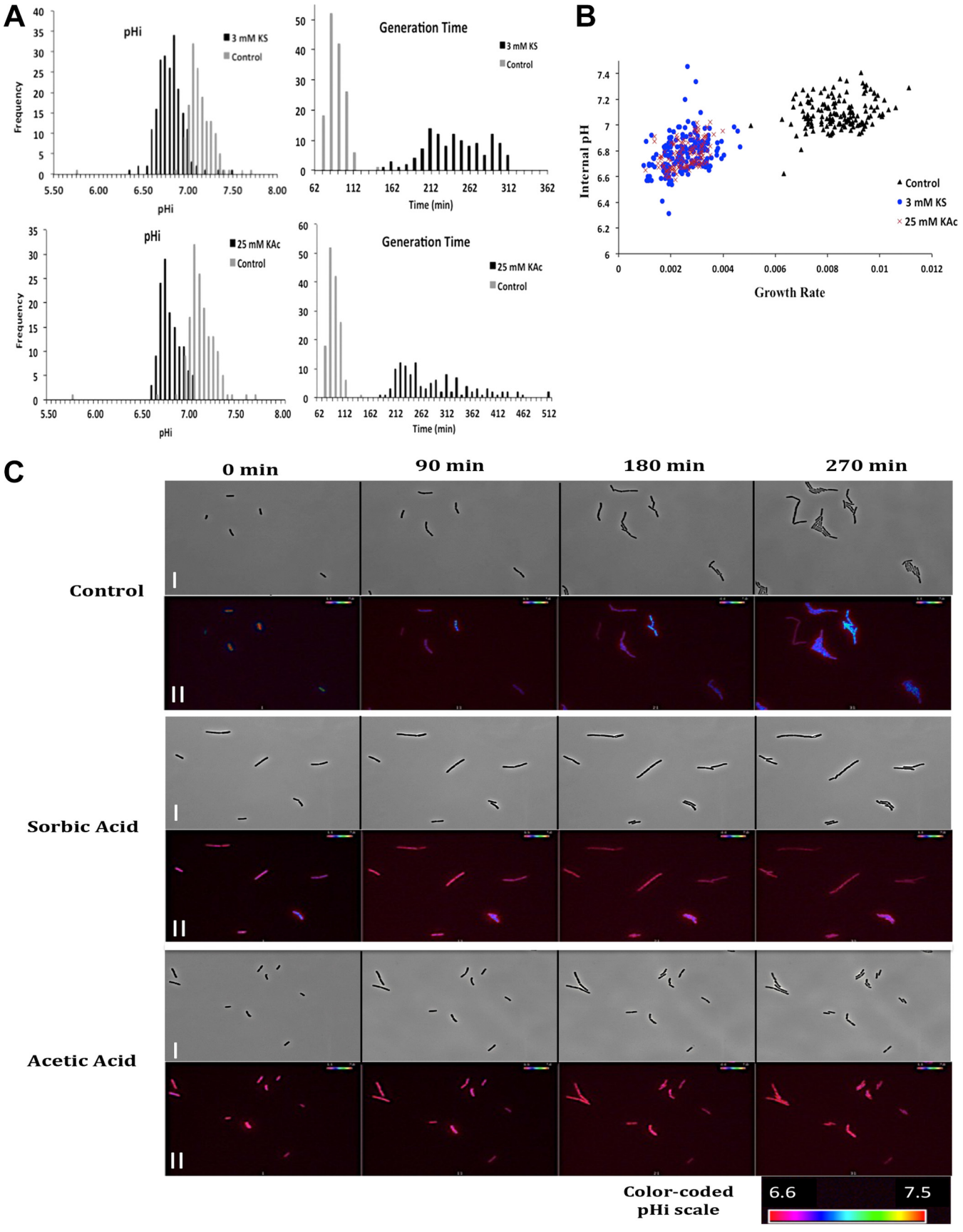

TABLE 3 Mean values and standard deviation of internal pH and generation time of individual *B. subtilis* PptsG-IpHluorin vegetative cells in the presence and absence of sorbic acid and acetic acid[a]

Parameter	Treatment (mean ± SD) (min) (*n*)[b]		
	None	Potassium sorbate	Potassium acetate
pH_i	7.20 ± 0.24 (151)	6.78 ± 0.14 (205)[c]	6.76 ± 0.11 (131)[c]
Generation time (min)	114 ± 21 (164)	304.63 ± 109.70 (109)[c]	286.13 ± 80.78 (122)[c]

[a] *B. subtilis* PptsG-IpHluorin vegetative cells were grown in MOPS medium stressed with or without 3 mM potassium sorbate and 25 mM potassium acetate.
[b] *n*, the amount of cells analyzed for pH_i and generation time determination are gathered from two (control, sorbic acid, and acetic acid) microscopy experiments and given in parentheses.
[c] Variance of the distributions between the stress and control experiment are significantly different ($P < 0.01$), and the mean of the distributions between the stress and control experiment are significantly different (*t* test, $P < 0.01$).

under the tested conditions. Next, cells were exposed to sequential pulses of light of two different wavelengths (390 nm and 470 nm for 100 and 30 ms, respectively) with 5-min or 10-min intervals between fluorescence measurements. Figure 3 also shows the effect of repeated exposure of cells to 390 nm and 470 nm excitation on the generation time of the *B. subtilis* PptsG-IpHluorin-expressing cells. Both conditions, i.e., 5-min and 10-min intervals, resulted in a slight increase in generation time (116 ± 3 min and 114 ± 21 min, respectively) without causing cell death (no cell lysis was observed while analyzing either of the incubations microscopically). We conclude that our settings are suitable for up to 5 h of pHi live imaging and went for the longer 10-min interval in further experiments.

Sorbic and acetic acid impact on pH_i and growth of *B. subtilis* cells. Sorbic and acetic acid have detrimental effects on bacterial cells. The two acids have a similar pK_a of 4.76, but sorbic acid is lipophilic, whereas acetic acid is hydrophilic in nature. Here, the effect of exposure at pH 6.4 to 3 mM potassium sorbate and 25 mM potassium acetate was studied in vegetative *B. subtilis* cells at the single-cell level. Figure 4 shows the effect of sorbic and acetic acids on the pH_i and generation time of *B. subtilis* PptsG-IpHluorin vegetative cells growing in microcolonies. In sorbic acid-stressed cells, the average internal pH of the microcolonies decreased from 7.2 to 6.8 (Fig. 4A and Table 3), and the generation time increased significantly (Fig. 4A and Table 3). In 25 mM potassium acetate-stressed cells, a similar trend in internal pH and increase in generation time were observed (Fig. 4A and Table 3). Figure 4B gives the correlation graph between the average internal pH of the microcolonies and generation time for control cells, as well as cells stressed with the two acids. PptsG-IpHluorin-expressing cells are typically lowered 50% in their growth rate by the addition of 3 mM potassium sorbate or 25 mM potassium acetate to liquid cultures while monitoring population-level pH_i (4). Here, growth rate inhibition by these concentrations of both weak organic acids is increased, and the observed standard deviation for the population is high. This might reflect some light sensitization by the weak organic acid stresses. However, we have also shown previously that in the MOPS-buffered defined medium used here, there is an ~30% increase in generation time of wild-type *B. subtilis* cells compared to liquid culture conditions (25). Hence, although we cannot exclude that under our live-imaging conditions, weak acid stress response may sensitize the PptsG-IpHluorin-expressing cells to light, it will not be the major response seen.

In conclusion, acid-stressed cells and control populations displayed significant differences in both pH_i and growth rate ($P < 0.001$). Figure 4C shows selected time points from movies (see Videos S1 to S3 and Table S1 in the supplemental material) of *B. subtilis* PptsG-IpHluorin vegetative cells in the presence and absence of 3 mM potassium sorbate and 25 mM potassium acetate, which are color-coded by their pH_i. Noticeably, as was observed previously in a study by van Beilen et al. (see Fig. 1b in reference 4), the pH_i of control cells started in some cells at values above 8, indicating a somewhat stalled metabolic activity at the onset of imaging. In this regard, we noted a clear batch variation between the two biological repeats shown. Growth rate and average colony pH_i calculations with Multichannel-SporeTracker were always performed from the time point at which a clearly detectable surface increase, i.e., growth, had resumed. pH_i was then generally ~7.5, values seen previously by van Beilen et al. in liquid populations (4, 20).

Lineage tracing of individual cells in microcolonies reveals pH_i heterogeneity. As noted in Materials and Methods, single *B. subtilis* cells grow and divide to form microcolonies. We observed that within a developing microcolony, the E_{390}/E_{470} fluorescence ratio of individual *B. subtilis* cells differs. This shows that there is heterogeneity in pH between individual *B. subtilis* cells in a microcolony at a given time point of culture. Figure 5 shows for control conditions a typical example of tracking individual cells, growing from a single cell up to a microcolony. It became clear that under those conditions, after a transient drop in pH_i presumably due to the increased levels of acetate made by the growing bacteria themselves (see, e.g., reference 4), individual bacteria are likely able to mount to various extents a response that allows them to finally

FIG 4 Analysis of *B. subtilis* PptsG-IpHluorin vegetative cells growing into microcolonies with Multichannel-SporeTracker shows that pH_i and generation time of sorbic acid- and acetic acid-treated cells are affected. (A) pH_i frequency distributions of microcolonies of sorbic acid- and acetic acid-stressed (black) as well as control (gray) *B. subtilis* PptsG-IpHluorin cells were calculated per 0.05 pH unit bin from data obtained in two biological repeats. Depicted are the frequency distributions as well as the generation times of *B. subtilis* PptsG-IpHluorin cell microcolonies exposed to 3 mM potassium sorbate and 25 mM potassium acetate at pH 6.4, respectively. (B) Growth rate versus pH_i of *B. subtilis* PptsG-IpHluorin cells growing in microcolonies for unstressed cells and cells stressed with sorbic acid and acetic acid. Between the acid-stressed cells and the control populations, both the mean and the variance of pH_i and growth rate are significantly different (*t* test, $P < 0.01$). (C) Still images at set time points of phase-contrast (I) and fluorescence data (II) showing growth and division of *B. subtilis* PptsG-IpHluorin vegetative control cells (top row) and cells grown in the presence of 3 mM potassium sorbate (middle row) and 25 mM potassium acetate (bottom row) at an external pH of 6.4. The acids were included in the agarose slides from the onset of the experiment. Imaging was done as described in Materials and Methods, with a 10-min illumination interval.

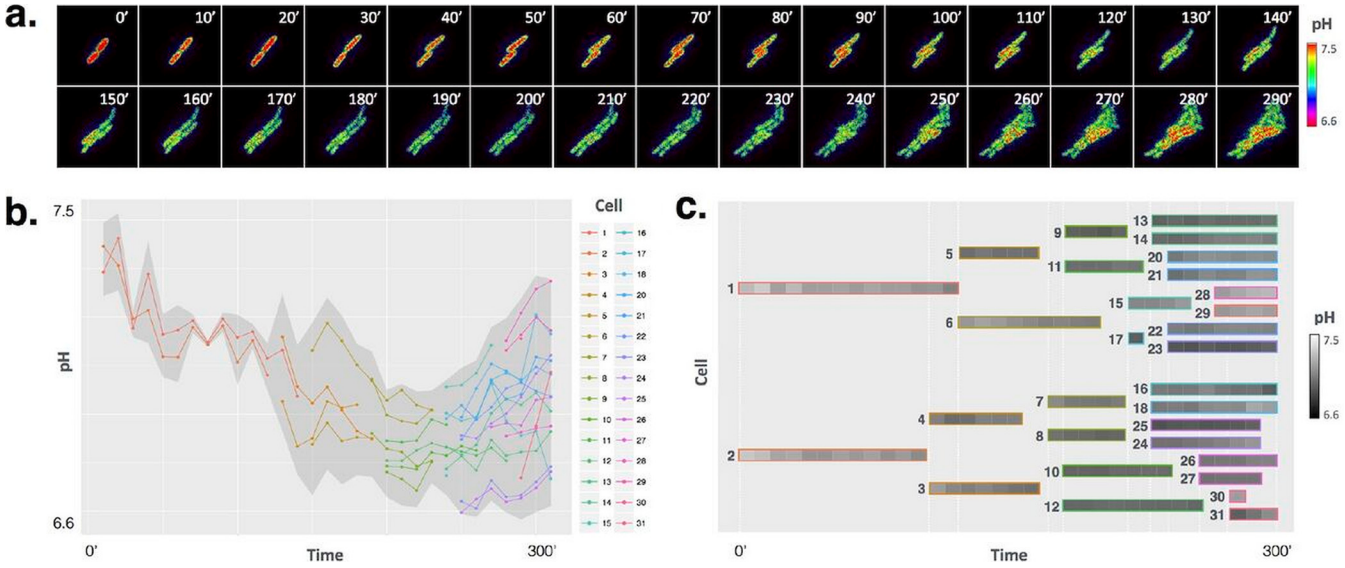

FIG 5 Time-resolved ratiometric image showing growth and division of a single *B. subtilis* PptsG-IpHluorin vegetative cell in the absence of stress at an external pH of 6.4. (a) Montage of the ratio image in which the color represents the pH. (b) The pH profiles of individual color-coded cells superimposed on the standard deviation of the mean signal of the entire microcolony in gray. (c) Lineage tracking and ratio changes in gray scale.

again raise their internal pH, albeit to various degrees. Such variation in pH_i is also observed for the cells that underwent intentional weak organic acid stress. This is true in particular for those exposed to sorbic acid (Fig. 4A and B). Strikingly, under conditions of 3 mM potassium sorbate stress, microcolonies emerged with pH_i values well within the range of those from control cells as well as values that were well below. While pH_i is clearly a major determinant of growth rate, it is definitely not the only one, certainly not under sorbic acid stress.

DISCUSSION

Here, we deployed a derivative of green fluorescent protein (GFP), IpHluorin, to probe at the single-cell level the pH_i of *B. subtilis* cells. The use of this genetically encoded reporter holds various advantages, such as inherent labeling, strong signal-to-noise ratio, and concentration independence. A potential disadvantage is its requirement for molecular oxygen, precluding its use in anaerobic species, such as *Clostridium* species.

Using *B. subtilis* cells stably expressing IpHluorin, we have established a robust microscopy-based assay for simultaneously measuring pH_i and generation time. We first tuned the imaging conditions so as to minimize phototoxicity. Subsequently, we established a calibration curve showing a strong correlation of the fluorescence ratio with the externally adjusted pH ranging from 5.5 to 8.5. Once optimized, we benchmarked our assay using two well-known weak acid preservatives, namely, sorbic and acetic acid. Also, to analyze the microscopy images, we developed a semiautomated image analysis tool based on the previously published SporeTracker (25), called the Multichannel-SporeTracker. This tool calculates the internal pH and the generation time of exponentially growing *B. subtilis* PptsG-IpHluorin-expressing vegetative cells. It allows us to monitor individual cells and subpopulations and deconvolute the population-level information at the single-cell level.

The analysis of the effect of sorbic acid and acetic acid on vegetative cells showed that at low concentrations of sorbic acid, the generation time increases with decreasing pH_i. Similar results were obtained from the analysis of acetic acid-treated cells, albeit at higher acid concentrations, and a wider distribution of generation times is seen. Thus, at the selected concentrations, the two acids reduce the pH_i and the growth rate to a similar extent. This result corroborates the notion that sorbic acid is the more effective preservative of the two. van Beilen et al. showed that sorbic acid is unable to recover pH_i during acid stress. These observations reflect the notion that sorbate acts as a classical uncoupler, which shuttles protons over the membrane, whereas acetate is believed to do this to a much lesser extent (4). The data of the study by van Beilen et al. show that sorbic acid has an effect on the membrane potential, while acetic acid carries only bulk volume protons across the membrane until steady state is reached, leaving $\Delta\psi$ relatively unaffected. In line with this, and in accordance with data previously obtained in yeast (reviewed by Orij et al. [17]), van Beilen et al. (4) showed that at the population level, growth rate and pH_i behavior in *B. subtilis* can be correlated. We now also demonstrate a similar correlation at the single-cell level, demonstrating that pH_i can be assessed as a good indicator of individual bacterial health. From this knowledge of pH_i, one could infer at the individual cell level the activity of metabolic pathways that are key to cellular energy conversion. Such data may be used by food microbiologists to feed contemporary models that aim at quantitatively predicting microbial food stability. This study suggests that heterogeneity at the individual cell level is prominent, with important implications for weak organic acid-based food preservation strategies. We can now, through lineage tracing, also start to verify mechanistically whether under long-term weak organic acid stress conditions, subpopulations of *Bacillus* cells arise that might be more able to restore their pH_i, hence explaining their better survival in foods and outgrowth potential to new (micro)colonies that can spoil foods. It may also be applied to the analysis of other potential food spoilage organisms, e.g., *Zygosaccharomyces bailii* (29).

In conclusion, our microscopy-based single-cell analysis technique effectively allows for gauging pH_i and relating it to generation time. In doing so, the method can provide further mechanistic insight into the principles of existing and novel food preservation strategies. The analysis can be extended to the ratiometric assessment of the dynamics of the pH_i of spores during germination and outgrowth. It will allow one to point out the phase where weak acids have a maximum effect and also could provide key information about the timing of weak organic acid action on individual germinating and outgrowing spores. This information can be coupled to risk management of the unwanted growth of bacteria in food and hence help the food industry combat food spoilage. An attractive platform for implementing such an assay would be a microfluidics-based lab-on-chip system (30). Such a platform allows for rapid measurement of pH_i values under dynamically changing conditions (change of medium types or supplements) coupled to monitoring of the dynamics of spore germination and outgrowth. This type of experiment should provide ways to deconvolute the population data with respect to the effects of different sequences of stresses on the germination and (out)growth efficiency of *B. subtilis* spores.

ACKNOWLEDGMENTS

Huub Hoefsloot and Chris de Koster are thanked for expert advice on statistics analyses.

Rachna Pandey was supported by the Erasmus Mundus program (EMECW 15) and the University of Amsterdam. Alexander Ter Beek was supported by a grant from the Dutch Foundation of Applied Sciences (STW 10431).

FUNDING INFORMATION

This work, including the efforts of Rachna Pandey, was funded by European Commission (EC) (EMECW 15). This work, including the efforts of Alexander Ter Beek, was funded by Nederlandse Organisatie voor Wetenschappelijk Onderzoek (NWO) (STW 10431). This work, including the efforts of Winnok H. De Vos, was supported by University of Antwerp (TTBOF/29267).

REFERENCES

1. **Shioi JI, Matsuura S, Imae Y.** 1980. Quantitative measurements of proton motive force and motility in *Bacillus subtilis*. J Bacteriol **144:**891–897.
2. **Krebs HA, Wiggins D, Stubbs M, Sols A, Bedoya F.** 1983. Studies on the mechanism of the antifungal action of benzoate. Biochem J **214:**657–663. http://dx.doi.org/10.1042/bj2140657.
3. **Mols M, Abee T.** 2011. *Bacillus cereus* responses to acid stress. Environ Microbiol **13:**2835–2841. http://dx.doi.org/10.1111/j.1462-2920.2011.02490.x.
4. **van Beilen JWA, Teixeira de Mattos MJ, Hellingwerf KJ, Brul S.** 2014. Sorbic acid and acetic acid have distinct effects on the electrophysiology and metabolism of *Bacillus subtilis*. Appl Environ Microbiol **80:**5918–5926. http://dx.doi.org/10.1128/AEM.01391-14.
5. **Holyoak CD, Stratford M, McMullin Z, Cole MB, Crimmins K, Brown AJP, Coote PJ.** 1996. Activity of the plasma membrane H^+-ATPase and optimal glycolytic flux are required for rapid adaptation and growth of *Saccharomyces cerevisiae* in the presence of the weak-acid preservative sorbic acid. Appl Environ Microbiol **62:**3158–3164.
6. **Bracey D, Holyoak CD, Nebevon Caron G, Coote PJ.** 1998. Determination of the intracellular pH (pH_i) of growing cells of *Saccharomyces cerevisiae*: the effect of reduced-expression of the membrane H^+-ATPase. J Microbiol Methods **31:**113–125. http://dx.doi.org/10.1016/S0167-7012(97)00095-X.
7. **Henriques M, Quintas C, Loureiro-Dias MC.** 1997. Extrusion of benzoic acid in *Saccharomyces cerevisiae* by an energy-dependent mechanism. Microbiology **143:**1877–1883. http://dx.doi.org/10.1099/00221287-143-6-1877.
8. **Piper P, Mahe Y, Thompson S, Pandjaitan R, Holyoak C, Egner R, Mühlbauer M, Coote P, Kuchler K.** 1998. The Pdr12 ABC transporter is required for the development of weak organic acid resistance in yeast. EMBO J **17:**4257–4265. http://dx.doi.org/10.1093/emboj/17.15.4257.
9. **Eklund T.** 1985. Inhibition of microbial growth at different pH levels by benzoic and propionic acids and esters of *p*-hydroxybenzoic acid. Int J Food Microbiol **2:**159–167. http://dx.doi.org/10.1016/0168-1605(85)90035-2.
10. **Ugurbil K, Rottenberg H, Glynn P, Shulman RG.** 1978. ^{31}P nuclear magnetic resonance studies of bioenergetics and glycolysis in anaerobic *Escherichia coli* cells. Proc Natl Acad Sci U S A **75:**2244–2248. http://dx.doi.org/10.1073/pnas.75.5.2244.
11. **Bulthuis BA, Koningstein GM, Stouthamer AH, van Verseveld HW.** 1993. The relation of proton motive force adenylate energy charge and phosphorylation potential to the specific growth-rate and efficiency of energy transduction in *Bacillus licheniformis* under growth condition. Antonie Van Leeuwenhoek **63:**1–16. http://dx.doi.org/10.1007/BF00871725.
12. **Magill NG, Cowan AE, Koppel DE, Setlow P.** 1994. The internal pH of the forespore compartment of *Bacillus megaterium* decreases by about 1pH unit during sporulation. J Bacteriol **176:**2252–2258.
13. **Breeuwer P, Drocourt J, Rombouts FM, Abee T.** 1996. A novel method for continuous determination of the intracellular pH in bacteria with the internally conjugated fluorescent probe 5 (and 6-)-carboxyfluorescein succinimidyl ester. Appl Environ Microbiol **62:**178–183.
14. **Leuschner RG, Lillford PJ.** 2000. Effect on hydration on molecular mobility in phase-bright *Bacillus subtilis* spore. Microbiology **146:**49–55. http://dx.doi.org/10.1099/00221287-146-1-49.
15. **Slonczewski JL, Fujisawa M, Dopson M, Krulwich TA.** 2009. Cytoplasmic pH measurement and homeostasis in bacteria and archaea. Adv Microb Physiol **55:**1–79, 317.
16. **Miesenbök G, De Angelis DA, Rothman JE.** 1998. Visualizing secretion and synaptic transmission with pH-sensitive green fluorescent proteins. Nature **394:**192–195. http://dx.doi.org/10.1038/28190.
17. **Orij R, Brul S, Smit GJ.** 2011. Intracellular pH is a tightly controlled signal in yeast. Biochim Biophys Acta **1810:**933–944. http://dx.doi.org/10.1016/j.bbagen.2011.03.011.
18. **Ullah A, Orij R, Brul S, Smit GJ.** 2012. Quantitative analysis of the mode of growth inhibition by weak organic acid in yeast. Appl Environ Microbiol **78:**8377–8387. http://dx.doi.org/10.1128/AEM.02126-12.
19. **Martinez KA, Jr, Kitko RD, Mershon JP, Adcox HE, Malek KA, Berkmen MB, Slonczewski JL.** 2012. Cytoplasmic pH response to acid stress in individual cells of *Escherichia coli* and *Bacillus subtilis* observed by fluorescence ratio imaging microscopy. Appl Environ Microbiol **78:**3706–3714. http://dx.doi.org/10.1128/AEM.00354-12.
20. **van Beilen JWA, Brul S.** 2013. Compartment-specific pH monitoring in *Bacillus subtilis* using fluorescent sensor proteins; a tool to analyse the antibacterial effect of weak organic acids. Front Microbiol **4:**157.
21. **Ter Beek A, Wijman JG, Zakrzewska A, Orij R, Smits GJ, Brul S.** 2015. Comparative physiological and transcriptional analysis of weak organic acid stress in *Bacillus subtilis*. Food Microbiol **45:**71–82. http://dx.doi.org/10.1016/j.fm.2014.02.013.
22. **Martínez-Muñoz GA, Kane P.** 2008. Vacuolar and plasma membrane proton pumps collaborate to achieve cytosolic pH homeostasis in yeast. J Biol Chem **283:**20309–20319. http://dx.doi.org/10.1074/jbc.M710470200.
23. **Orij R, Postmus J, Ter Beek A, Brul S, Smits GJ.** 2009. *In vivo* measurement of cytosolic and mitochondrial pH using a pH-sensitive GFP derivative in *Saccharomyces cerevisiae* reveals a relation between intracellular pH and growth. Microbiology **155:**268–278. http://dx.doi.org/10.1099/mic.0.022038-0.
24. **Kort R, O'Brien AC, van Stokkum IHM, Oomes SJCM, Crielaard W, Hellingwerf KJ, Brul S.** 2005. Assessment of heat resistance of bacterial spores from food product isolates by fluorescence monitoring of dipicolinic acid release. Appl Environ Microbiol **71:**3556–3564. http://dx.doi.org/10.1128/AEM.71.7.3556-3564.2005.
25. **Pandey R, Ter Beek A, Vischer NOE, Smelt J, Brul S, Manders EMM.** 2013. Live cell imaging of germination and outgrowth of individual *Bacillus subtilis* spores; the effect of heat stress quantitatively analyzed with SporeTracker. PLoS One **8:**e58972. http://dx.doi.org/10.1371/journal.pone.0058972.
26. **Back P, De Vos WH, Depuydt GG, Matthijssens F, Vanfleteren JR, Braeckman BP.** 2012. Exploring real-time *in vivo* redox biology of developing and aging *Caenorhabditis elegans*. Free Radic Biol Med **52:**850–859. http://dx.doi.org/10.1016/j.freeradbiomed.2011.11.037.
27. **Motulsky H, Christopoulos A.** 2004. Fitting models to biological data

using linear and nonlinear regression. A practical guide to curve fitting. Oxford University Press, Oxford, United Kingdom.
28. **Hoebe RA, Van Oven CH, Gadella TW, Jr, Dhonukshe PB, Van Noorden CJ, Manders EM.** 2007. Controlled light-exposure microscopy reduces photobleaching and phototoxicity in fluorescence live-cell imaging. Nat Biotechnol **25:**249–253. http://dx.doi.org/10.1038/nbt1278.
29. **Dang TD, De Maseneire SL, Zhang BY, De Vos WH, Rajkovic A, Vermeulen A, van Impe JF, Devlieghere F.** 2012. Monitoring the intracellular pH of Zygosaccharomyces bailii by green fluorescent protein. Int J Food Microbiol **156:**290–295. http://dx.doi.org/10.1016/j.ijfoodmicro.2012.03.028.
30. **Dutse SW, Yusof NA.** 2011. Microfluidics-based lab-on-chip systems in DNA-based biosensing: an overview. Sensors (Basel) **11:**5754–5768. http://dx.doi.org/10.3390/s110605754.
31. **Kitko RD, Cleeton RL, Armentrout EI, Lee GE, Noguchi K, Berkmen Melanie B, Jones BD, Slonczewski JL.** 2009. Cytoplasmic acidification and the benzoate transcriptome in *Bacillus subtilis*. PLoS One **4:**e8255. http://dx.doi.org/10.1371/journal.pone.0008255.

AMERICAN SOCIETY FOR MICROBIOLOGY | Applied and Environmental Microbiology®

ERRATUM

Erratum for Pandey et al., "Intracellular pH Response to Weak Acid Stress in Individual Vegetative *Bacillus subtilis* Cells"

Rachna Pandey,[a] Norbert O. E. Vischer,[a] Jan P. P. M. Smelt,[a] Johan W. A. van Beilen,[a] Alexander Ter Beek,[a] Winnok H. De Vos,[b,c] Stanley Brul,[a] Erik M. M. Manders[d]

Molecular Biology and Microbial Food Safety, SILS, University of Amsterdam, Amsterdam, The Netherlands[a]; Department of Veterinary Sciences, Laboratory of Cell Biology and Histology, Antwerp University, Antwerp, Belgium[b]; Department Molecular Biotechnology, Cell Systems and Imaging Group, Ghent University, Ghent, Belgium[c]; Van Leeuwenhoek Centre for Advance Microscopy, SILS, University of Amsterdam, Amsterdam, The Netherlands[d]

Volume 82, no. 21, p. 6463–6471, 2016, https://doi.org/10.1128/AEM.02063-16. Page 6470, Acknowledgments: The first paragraph should include the sentence "Gertien Smits is thanked for her ground-laying work, as well as the many stimulating discussions on the measurement of intracellular pH and its role in cell growth."

Page 6470: References 16 through 18 should read as follows.

16. Miesenböck G, De Angelis DA, Rothman JE. 1998. Visualizing secretion and synaptic transmission with pH-sensitive green fluorescent proteins. Nature 394:192–195. https://doi.org/10.1038/28190.

17. Orij R, Brul S, Smits GJ. 2011. Intracellular pH is a tightly controlled signal in yeast. Biochim Biophys Acta 1810:933–944. https://doi.org/10.1016/j.bbagen.2011.03.011.

18. Ullah A, Orij R, Brul S, Smits GJ. 2012. Quantitative analysis of the mode of growth inhibition by weak organic acid in yeast. Appl Environ Microbiol 78:8377–8387. https://doi.org/10.1128/AEM.02126-12.

Citation Pandey R, Vischer NOE, Smelt JPPM, van Beilen JWA, Ter Beek A, De Vos WH, Brul S, Manders EMM. 2017. Erratum for Pandey et al., "Intracellular pH response to weak acid stress in individual vegetative *Bacillus subtilis* cells." Appl Environ Microbiol 83:e00861-17. https://doi.org/10.1128/AEM.00861-17.